Applied Energy 282 (2021) 116160

Contents lists available at ScienceDirect

Applied Energy

journal homepage: www.elsevier.com/locate/apenergy

Temporal city-scale matching of solar photovoltaic generation and electric vehicle charging

Ulrich Fretzen, Mohammad Ansarin *, Tobias Brandt

Rotterdam School of Management, Erasmus University, Rotterdam, Netherlands

GRAPHICAL ABSTRACT

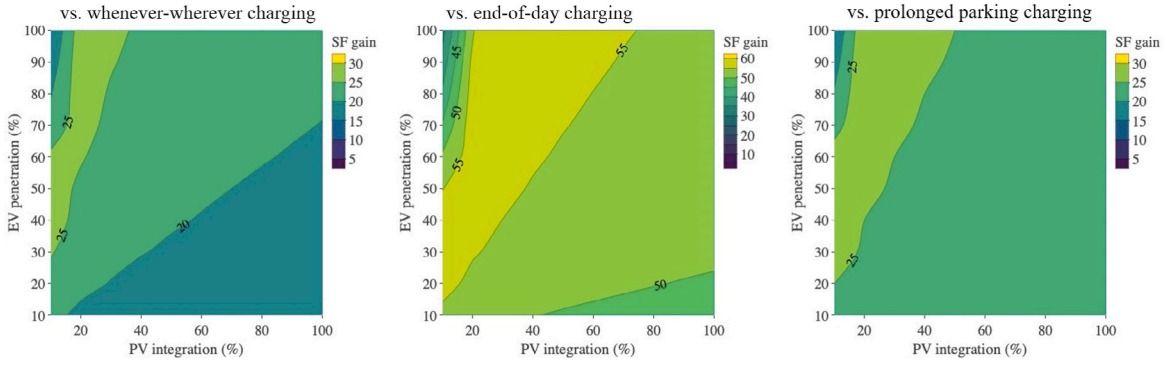

ARTICLE INFO

Keywords:
Renewable energy
Electric vehicles
Solar panels

ABSTRACT

The number of electric vehicles (EVs) and solar photovoltaic panels (PVs) are rapidly increasing in many power grids. An important emerging challenge is managing their less desirable consequences (e.g. grid instability and peak load), particularly in urban environments. We present a solution that matches the temporal nature of PV generation and EV charging. This solution is a simple coordination strategy for EV charging which minimally affects EV availability for drivers while maximizing the PV electricity generation absorbed by EV batteries. The strategy is benchmarked with high-resolution data from a medium-sized European city. We find that this coordination provides large benefits compared to commonly-observed uncoordinated charging patterns across seasons and PV and EV integration levels. With charging coordination, almost 71%–92% of the EV charging load can be provided by solar panels in the summer. However, winter's lower solar irradiance results in a larger range of possibilities (13%–76%), with the exact value depending on the combination of PV and EV integration level. The gains compared to uncoordinated charging are generally highest in winter and similarly vary based on PV and EV integration levels (from 5 to 63 percentage points). Additionally, these benefits do not appear to come at a significant cost to EV availability for drivers.

1. Introduction

Environmental concerns about climate change and pollution have created widespread interest in replacing coal- and natural gas-based electricity generation with cleaner alternatives. While the burning of fossil fuels is controllable and predictable in its electricity generation, renewable energy sources (RES), such as solar photovoltaic panels (PV), are weather-dependent and less easily manageable [1]. Thus, a significant issue in the renewable energy transition has been the supply-side change in predictability and controllability [2,3].

On the demand side, similar environmental concerns have encouraged a transition from transportation based on fossil fuels to one based on electricity and (ultimately) renewable energy sources [4]. While the

* Corresponding author.
E-mail address: ansarin@rsm.nl (M. Ansarin).

https://doi.org/10.1016/j.apenergy.2020.116160
Received 11 August 2020; Received in revised form 22 October 2020; Accepted 28 October 2020
Available online 18 November 2020

Table 1
Nomenclature.

Label	Unit	Description
PV	N/A	Photovoltaic panel
EV	N/A	Electric vehicle
RES	N/A	Renewable energy sources
pp	N/A	percentage points
GCR	–	Ground Coverage Ratio
p	–	State transition probability
t	min	Time
S	–	EV state space
$p_{j\to k}$	–	Vehicle transition probability from state j to state k
N	–	Markov driving state transition matrix
E	kWh	EV battery energy state
C^{ψ}	kW	Charging power for event ψ
d	km	Travel distance
η	kWh/km	Electricity consumption per travel distance
L(t)	kW	PV generation
P(t)	kW	EV charging load
M(t)	kW	PV generation coincidence with EV charging load
SF	–	Solar fraction
LF	–	Load fraction

technology has existed since the early days of electricity [5], electric vehicles (EV) have recently become viable alternatives to vehicles using internal combustion engines [6]. Consequently, EV counts are expected to reach 125 million by 2030 [7], pushing a rapid and large-scale increase in electricity demand in many regions.

As EV electricity demand grows, charging with cleanly-generated electricity becomes vital for achieving positive environmental effects from EV adoption [4]. Similarly, EV charging has potential for mitigating the intermittent supply issues of RES and thus smoothing their grid integration [8,9]. Various studies on RES have examined the interaction between wind generation and EVs; however, the synergistic potential between solar energy and EVs is less researched [8]. Some studies have analyzed PV potential or EV charging separately, with few focusing on the intersection between the two technologies [10]. Shepero et al. [10] review various studies that have investigated the potential to satisfy EV energy needs with PV generation [11–13]. Many studies limit themselves to small-scale matching of EVs and PVs [14–16]. Expanding the analysis of the alignment between PV generation and EV charging to a city-wide scale is critical for understanding the impact of these technologies on urban power grids. However, prior city-wide studies had low granularity [17,18], disregarded temporal matching [12] and/or oversimplified assumptions (see Shepero et al. [10],Wu et al. [19] for details). These issues drastically limit the realism and geographic applicability of their results and stress the lack of conclusive high-resolution spatiotemporal studies on the synergistic potential of PV generation and EV charging [12].

Additionally, the papers mentioned in the prior paragraph match PV generation with uncoordinated EV charging behavior [13]. Although Good et al. [13] ascribe rooftop PV yields a considerable potential in covering EV charging loads, they neglect the flexibility of EV charging, whose patterns can be matched with PV generation [20]. Such coordinated EV charging has been attributed immense potential to address the generation uncertainty of PV [21]. Studies on grid stability have found charging coordination to be a crucial mitigator of grid congestion [22]. However, the realism of the smart charging methodologies in previous studies has been questioned [23]. Further, the developed charging schemes are compromising the EV owners' flexibility and are thus not realistically applicable [24].

This study represents a comprehensive simulation which integrates state of the art simulation techniques for both PV generation and EV use patterns to quantify the added benefit of coordinated charging in a multitude of possible scenarios in a representative medium-sized Western European city. While independent assessments and models of EV charging and PV generation have proliferated in recent years [10], granular models that integrate large scale real-life data sets at city scale are still scarce. Previous research has among others failed to consider coordinated charging [13], have not assessed the impact of coordination on grid stability instead of renewable utilization [22], limited its scope to single instances of charging stations [21] or failed to establish sufficient time resolution [17]. Our study addresses the aforementioned shortcomings. The study is also novel in its realism, as it defines EV driver discomfort as a critical assessment criterion for the coordinated charging scheme. Specifically, the modeling and granularity allows the study to determine the exact traveling delays due to coordinated charging, thus scrutinizing the proposed methodology with regard to one of the most relevant hindrances yet commonly neglected assessment criteria for coordinated EV charging with PV generation [24]. Thus, our study provides actionable insights and informs decision-making of electricity distributors, consumers, charging station and system operators, and public institutions.

In this paper, we demonstrate the detrimental impact of uncoordinated charging and extend existing research by quantifying the benefits of coordinated charging. In a first step, geospatial modeling provides potential rooftop PV generation patterns. Next, EV usage patterns are modeled with real-world transportation information. Based on this usage, multiple EV charging strategies with different heuristics and coordination strategies are compared with respect to their synergies with PV generation. We use data from Rotterdam, a medium-sized Dutch city, to quantify the model's results.

In the following pages, we first review our methods and data (Section 2). We then describe the calculations of PV generation (Section 3) and EV driving patterns (Section 4). Following a description of uncoordinated charging results (also in Section 4), we present coordinated charging results in Section 5. We conclude by discussing some policy implications and potential future work in Section 6.

2. Methods and data

2.1. Solar panel generation

2.1.1. Panel installation characteristics

To calculate total electricity generation from solar panels in the city, we first calculate the total surface area available for solar PV installations (See Table 1 for full nomenclature.). Prior research [25–27] has used light detection and ranging data to create a 3-dimensional city-wide model. We used such data with a point density of 4 points per m^2 for the city of Rotterdam, Netherlands.[1] Such a model allows us to differentiate roofs based on the suitability of various PV installation setups. For example, some rooftops may be slanted or obstructed, making them less suitable for PV installations. For tilted rooftops, similar to Good et al. [13] we assume that tilt azimuths are uniformly distributed and fall into seven azimuth values, from 90 degrees (east) to 270 degrees (west). North-facing roofs (azimuths of 270 to 90 degrees) are removed due to suboptimal performance from own-roof shading. We use an optimal tilt angle of 35 degrees based on solar irradiance patterns in Rotterdam.

For flat rooftops, we assume both south-facing and east–west facing panel setups. South-facing panels optimize power generation per panel, but exhibit a low ground coverage ratio (GCR). Alternatively, east–west facing panels, which gained popularity more recently, show higher GCR values despite suboptimal azimuths and thus power generation. This setup is also believed to create power generation that aligns better with demand peaks, thus improving grid stability and reliability [28,29]. In this paper, we consider both setups for flat rooftops. In the main text, we report on results for south-facing panels. A description of results for east–west facing panels (which are similar) is in Appendix 7.3.

[1] This proprietary data was obtained from Sobolt. More details at https://www.sobolt.com/.

Both rooftop panel setups are assumed to have fixed panel installations. For south-facing panels, self-shading due to higher panel tilts and limited rooftop areas is a significant issue. Recent decreases in solar panel costs have led to favoring increased panel numbers, reducing inter-row spacing thereby increasing GCR while lowering panel tilt in order to mitigate panel self-shading [30]. Thus, individual panels produce less electricity, whereas the entire rooftop's production is maximized. Based on industry practice in Rotterdam, we assume a tilt angle of 10 degrees and 53 centimeters of inter-row spacing, resulting in a GCR of 0.66.

Unlike south-facing panels, east–west facing panels are subject to negligible shading from other panels. Hence, only 10% of rooftop space is assumed empty for maintenance purposes, while remaining space is covered by panels with a GCR of 1.035. Panels are assumed to be split equally between azimuths of 90 and 270 degrees with tilt angles of 15 degrees, similar to Good et al. [13].

2.1.2. Solar irradiance

To find horizontal solar irradiance per hour, we use Aguiar et al. [31]'s method based on Markov transition matrices to generate local per-minute irradiance levels from aggregate climate data. We use this methodology to find solar irradiance for sample weeks in winter (December), spring (March), and summer (June).

This horizontal irradiance is transformed to direct and diffuse solar irradiance on each PV panel. The former is translated directly based on tilt and azimuth. Diffuse solar irradiance is split between anisotropic and isotropic values, which is then transferred to direct irradiance based on the model of Mckay [32].

The irradiance received by each photovoltaic module may be further reduced by losses from dirtiness and incidence angle. The model from Martin and Ruiz [33] is used here to find the final real irradiance value per solar panel.

2.1.3. Solar PV panel generation

Based on panel characteristics and per-panel irradiance rates, we calculate total electricity generation per minute per panel for each sample period (one week in spring, summer and winter). Similar to Byrne et al. [34], we assume 20% module efficiency (i.e. efficiency of energy transformation from solar irradiance to electricity). Likewise, as in Byrne et al. [34], Good et al. [13],Ko et al. [26], we assume negligible losses from converters and other equipment and battery charging.

2.2. Electric vehicle charging

We find the electricity demand for each EV at each time with a three-step process. First, we simulate EV driving patterns based on historical driving data. Second, we transform these driving patterns to the EV's battery charge state. Third, we determine the charging pattern based on the charging strategy.

2.2.1. Simulating EV driving patterns

The timing and destination of EV rides are simulated with a Markov chain model. Vehicle travel generally has a diurnal pattern, thus requiring a non-homogeneous Markov model [35]. Such a model was similarly used in Good et al. [13],Widén et al. [36],Soares and Lopes [37],Shepero and Munkhammar [38]. Similar to [13,38] the parking states of EVs are distinctly defined as "Home", "Work" and "Other". Unlike [13,38], this study adds a "Driving" state to account for traveling times. Thus, the driving state, D, accounts for cars that are currently traveling between any of the parking states. Together with the parking states, this represents the state space, S. These states are shown with the subscripts $\{H, W, O, D\}$. The transition probability between two states can then be expressed as

$$p^t_{j\to k} = P(E^t_k | E^{t-1}_j) \tag{1}$$

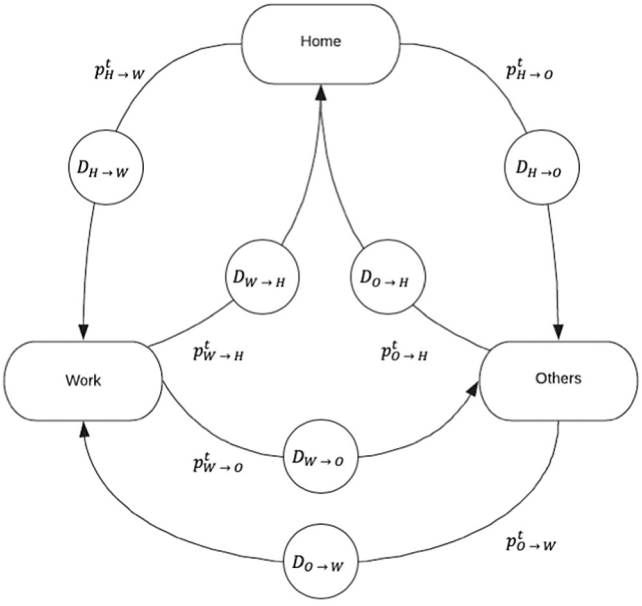

Fig. 1. Conceptual visualization of transitions between locations for EV state space.

where p represents the transition probability of a car transitioning from state j into state k, at time t.

A temporal resolution of one minute is selected in order to most accurately reflect traveling times, energy consumption and ultimately charging load. Thus, a Markov transition matrix can be drawn up for every minute of the day:

$$N_t = \begin{pmatrix} p^t_{H\to H} & p^t_{H\to W} & p^t_{H\to O} \\ p^t_{W\to H} & p^t_{W\to W} & p^t_{W\to O} \\ p^t_{O\to H} & p^t_{O\to W} & p^t_{O\to O} \end{pmatrix} \tag{2}$$

The driving distance and timing depend on the specific combination of origin and destination. The driving state of an EV transitioning from locations j to k can thus be expressed as:

$$D^t_{j\to k} \tag{3}$$

The state space and the associated Markov chain transition probabilities between location states are visualized in Fig. 1. Self-transitions for EVs that remain within the location state at a certain point in time, t, are not depicted.

Altogether, 2880 transition matrices (2 × 1440 min per day) are created to reflect the particular transition probabilities at every minute of the day during the week and on the weekend. The matrices are adopted from Shepero and Munkhammar [38], which based the transitions on Swedish travel data. Although the underlying travel data has been obtained in a different geography, namely Sweden, the overall travel patterns in Rotterdam are not expected to differ significantly, since people in the Netherlands can be expected to go home, to work, or to other locations in a similar pattern [13].

Initially all vehicles are located at home [18]. Subsequent night time locations depend on the transition matrices. In contrast to some prior research [18], including a driving state allows us to model non-instant transitions, thus accurately modeling real-life driving times.

The actual traveling distance, as well as traveling duration, are sampled from a subset of the Dutch Mobility Panel depending on the origin and the destination of the trip.[2] This data comprises 194,477 travel instances for which traveling destinations, motives, distances, and traveling times are recorded. The following criteria were used to exclude trips from the dataset:

[2] More details at https://www.mpndata.nl/.

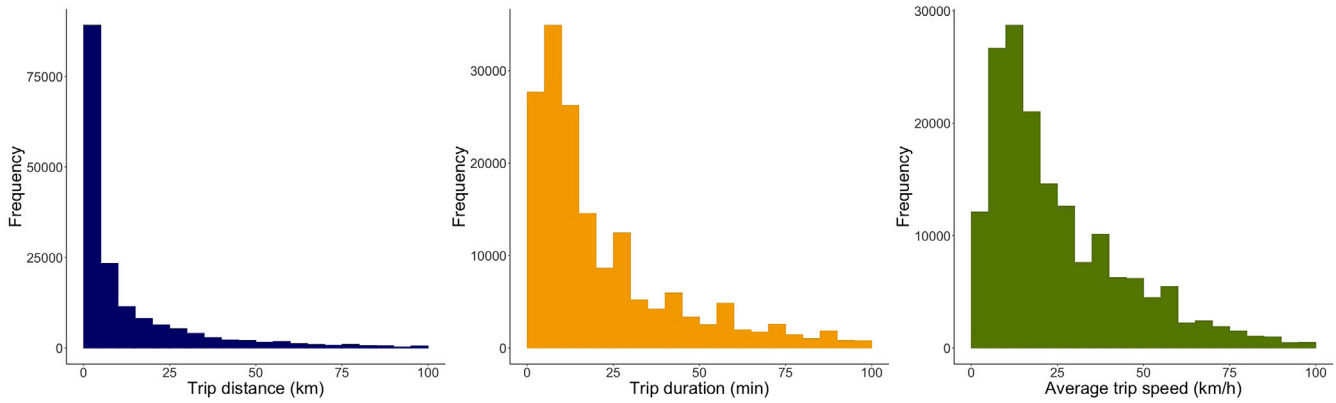

Fig. 2. Distribution of travel distance (l), duration (c), speed (r).

Table 2
Overview of charging strategies.

Strategy	Temporal constraint	Locational constraint
(1) Whenever, wherever	None	None
(2) End-of-day	After the last trip of day	At home
(3) Prolonged parking	Parking time > 120 min	None
(4) Coordinated with PV generation	None	None

1. Records without recorded travel distance (13,557) and records with traveling distances below 300 m (7035).
2. Trips with negative traveling times (25).
3. Records with distances longer than 150 km (1577), as they do not reflect the typical commute in the Netherlands.
4. Trips with a duration above 300 min (438), as such delays exceeds the obstructions incurred in usual traffic jams.
5. Trips with average speeds of above 120 km/h (410) and below 2 km/h (1720).

After cleaning, the data comprises 169,715 travels instances. A distribution of trip travel distance, trip duration and trip average driving speed is provided in Fig. 2. Travel distance follow an exponential distribution with a majority below 10 km. This distribution appears suitable to reflect the daily commutes of people living in a mid-size city. Traveling duration and traveling speed follow a Poisson distribution where trips under 15 min are the most common. However, a sizeable long tail reflects traveling journeys of 45 min and more. Common average speeds are between 10 to 25 km/h, reflecting the congestion within a midsize city.

By sampling trips with distinct traveling times and distances, each car can be assigned its own traveling speed. In this way, EV consumption per trip is based on the distance traveled within a certain time interval and independent from time. Consequently, traveling patterns become more realistic as opposed to previous studies, which assumed fixed velocities [29].

Based on this model, the travel patterns of 1,000 cars are simulated and subsequently extrapolated according to the EV penetration rate of a scenario (similar to Rassaei et al. [20]). Simulating a higher number of travel patterns provided negligible ($\leq$ 1%) change in EV load and final results.

2.2.2. Battery charge state

We use the travel patterns for the EVs to find each EV's battery charge state at each time.

In line with Grahn et al. (2013) and Good et al. (2018), the energy state E (kWh) of a vehicle's battery at a given time t can be represented by :

$$E^t = \begin{cases} E^{t-1} + C^{\psi} \times \Delta t \\ E^{t-1} - d \times \eta \\ E^{t-1} \end{cases} \quad (4)$$

C^{ψ} represents the charging power in kW that is used for charging event ψ, d is the travel distance in km, and η represents electricity consumption in kWh per km.

Our assumptions about the EV battery consist of the following:

1. EV Battery capacity has previously been assumed to be a truncated normal distribution of values [37] or a singular value [11,29]. Here we assume an EV fleet consisting of short/medium and long-range variants. Average battery sizes of 38 kWh and 72.5 kWh respectively were chosen from specifications for the most common EVs in the Netherlands (Nissan Leaf and Tesla Model S, respectively [39]). Similar to Soares and Lopes [37], these values are used to draw actual battery sizes from a truncated Gaussian distribution for each variant.
2. EV battery charge consumption was modeled as a kWh/km energy consumption rate obtained from a truncated normal distribution [37]. The distribution means were set separately for short/medium and long range EVs as 0.165 and 0.175 kWh/km, respectively.
3. Regarding charging speed, we chose a uniform value for all vehicles. This assumptions mirrors those of past research [12,18]. In the Netherlands, most public charging stations have a charging rate of 11kW, which is used here [40]. However, if a car is charged "on-the-go", the charging rate is assumed to be similar to those of Dutch fast-charging stations, i.e. 44 kW [39]. This aligns with the modeling choices of Soares and Lopes [37].
4. The initial state-of-charge of each EV at the beginning of each sample week is assumed to be equal to its maximum capacity for each EV. This is similar to most past studies (e.g. [18]).

We use this battery model to transform EV energy needs to grid charging.

2.3. EV charging strategies

Regaining the energy used for transportation depends on when charging the EV is possible. The available opportunities for EV charging depend on our assumed strategy. We consider three uncoordinated strategies which match those of past research. We add a coordinated strategy, designed to match solar PV generation with charging opportunities. (See Table 2.)

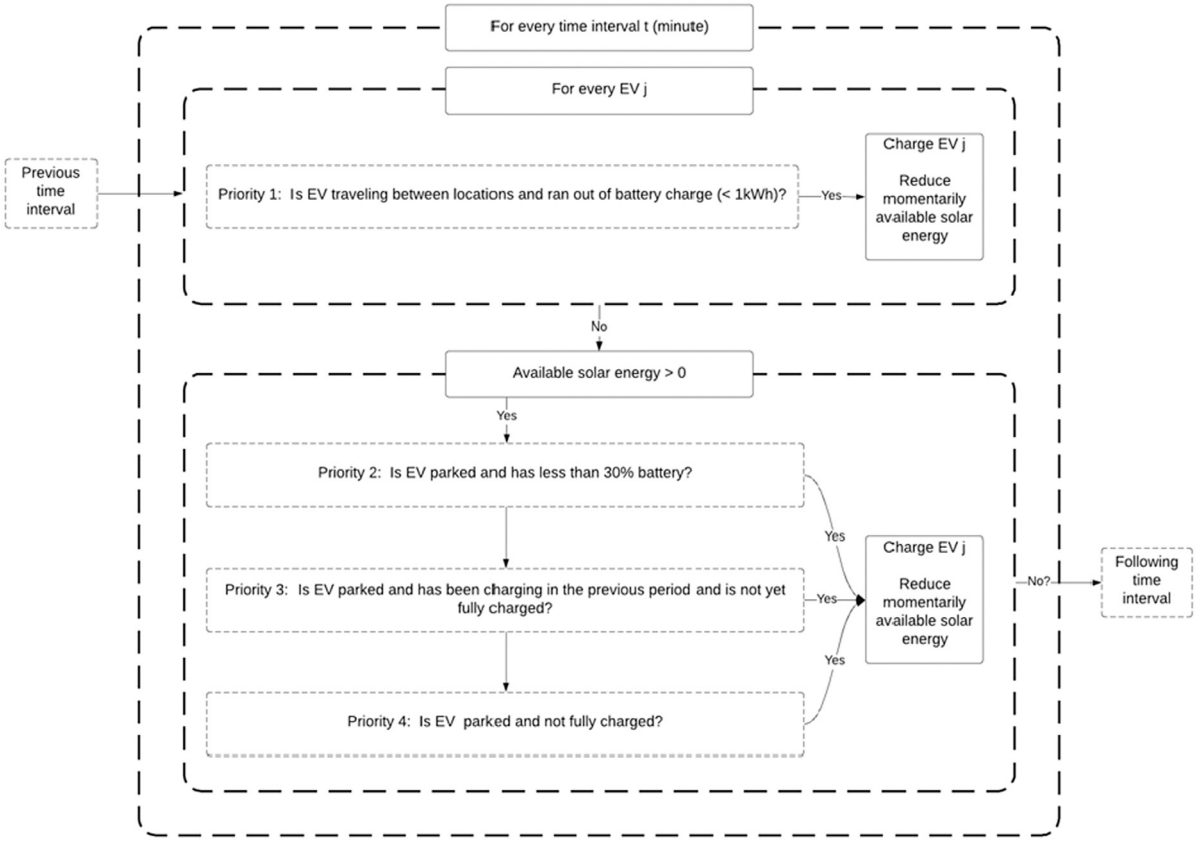

Fig. 3. Visualization of hierarchical charging algorithm.

1. *Strategy 1: Whenever, wherever* The first strategy does not impose any temporal or spatial restrictions on EV charging. Thus, EV owners are assumed to charge their parked EV without temporal constraints (whenever) and without locational constraints (wherever). This strategy has been identified by Soares and Lopes [37],Denholm et al. [41] and generally shifts charging load close to the actual discharge of the battery.
2. *Strategy 2: End-of-day* The second strategy simulates charging depending on the subsequent travel intentions of the individual EV driver. It models charging after the EV owner has parked his car at home after the last trip of the day. Thus, charging is limited to home charging, while the time of charging varies depending on the travel pattern of a specific day. This strategy is suggested as a suitable approximation of uncoordinated charging, e.g. in Falahati et al. [42].
3. *Strategy 3: Prolonged Parking* The third strategy models charging based on the duration of every parking instance. No spatial limitations are imposed on charging facilities, thus, charging is assumed to take place in all locations. However, charging is set to occur only in cases when the parking duration of an EV exceeds two hours. In this way, the model reflects the tendency to charge only during longer parking sessions [43].
4. *Strategy 4: Solar-dependent* The fourth strategy reflects the trend towards smart charging strategies. As opposed to other strategies focused on financial optimization and grid stability, this strategy explores the ability to shift charging load depending on the immediate availability of locally generated solar energy [44]. Thus, this strategy's objective is to simultaneously maximize solar fraction and load fraction subject to the EV and PV integration levels of the respective integration scenario. A visualization of the hierarchical charging algorithm is depicted in Fig. 3. In addition, if such energy is not available for charging prior to a next-day driving event, extra charging is scheduled at night at a randomly chosen time between 10PM and 4AM. Such hierarchical smart charging methodologies and control structures, which prioritize EVs based on an underlying algorithm, have been assigned increasing potential [45,46].

Across all four strategies the model allows for impromptu charging during a drive. As opposed to other studies which model the battery discharge of an imaginary unlimited battery [13] or assume battery charge to last for all trips [47], our study allows EVs to deplete their battery during a ride. We assume whenever a car battery runs out of energy during a trip, it is charged to 30% capacity at a 44 kW charging rate [39]. Due to the increasing density of the Dutch EV charging system, an additional detour for charging is not considered. This model is similar to Soares and Lopes [37] who assumed a depleted EV battery is charged for 15 min at 40 kW.

2.4. Scenario analysis

We focus here on the matching of solar PV electricity generation and EV charging. To this end, we consider two metrics from two separate perspectives.

The first, solar fraction, considers the extent to which EV charging load can be covered by PV electricity generation. Based on Luthander et al. [48], Munkhammar et al. [49], Good et al. [13],

$$SF = \frac{\int_{t_1}^{t_2}(M(t)dt)}{\int_{t_1}^{t_2}(L(t)dt)} \tag{5}$$

where $M(t)$ is the instantaneously coinciding part of the PV energy profile, $P(t)$, and the EV charging load profile, $L(t)$, defined as

$$M(t) = min(L(t), P(t)). \tag{6}$$

Fig. 4. PV Suitability in a sample region of Rotterdam, Netherlands.

Table 3
Overview of Scenarios.

Factor	Modeled instances
Season	Winter, Spring, Summer
PV integration (%)	10, 20, 30, 40, 50, 60, 70, 80, 90, 100
EV penetration (% of suitable area)	10, 20, 30, 40, 50, 60, 70, 80, 90, 100
Charging strategy	3 uncoordinated, 1 coordinated strategy
PV orientation on flat rooftops	south-facing and east–west-facing arrays

The second metric, load fraction, indicates the amount of solar generation that is absorbed by EV charging. Also following from Munkhammar et al. [49], Good et al. [13],

$$SF = \frac{\int_{t_1}^{t_2}(M(t)dt)}{\int_{t_1}^{t_2}(P(t)dt)} \tag{7}$$

The solar and load fractions are assessed for multiple scenarios. These scenarios vary in five dimensions, listed in Table 3. First, three sample weeks in spring, summer, and winter seasons are considered, due to each season's varying transportation and generation patterns. Second, PV integration levels are assessed from 0% to 100% of identified rooftops being used for solar panels (the current rate of Rotterdam rooftops using solar panels is 2.2% [50]). Third, EV integration levels are considered from none to all applicable transportation needs being covered by the EV fleet. Fourth, scenarios differ based on which charging strategy is used. Lastly, we separately considered both south-facing and east–west facing PV panels for flat rooftops.

3. City-wide solar photovoltaic generation

A model sample as well as rooftop PV suitability values are displayed in Fig. 4. This model is used to match PV panel installations with suitable rooftop areas. The total suitable area of Rotterdam amounts to 11.57 km^2, a value higher than for Dutch cities of comparable size due to Rotterdam's high ratio (75%) of flat roofs.

Based on suitable rooftop areas and solar irradiance levels, we calculate the potential PV generation per hour (details in Methods). Table 4 shows the total annual PV generation per level of integration in the energy system. For flat roofs, panels can be installed in both south and east–west configurations. The east–west panel setup consistently leads to higher overall energy output, despite having a lower energy output per installed m^2 of panel. This is mainly a consequence of the east–west setup's higher GCR.

Table 4
Annual electricity generation for scenarios with south and east–west-facing panels on flat roofs in GWh.

Integration Level	South	East–West	South per m^2	East–West per m^2
10%	196.6	231.7	226.6	211
20%	393.3	463.3	226.6	211
30%	589.9	695	226.6	211
40%	787.7	927.8	226.9	211.3
50%	986	1,161.1	227.2	211.6
60%	1,177.6	1,387.8	226.1	210.7
70%	1,369.3	1,614.5	225.4	210.1
80%	1,560.9	1,841.2	224.8	209.7
90%	1,747.5	2,062.7	223.7	208.8
100%	1,931.4	2,281.7	222.5	207.9

4. EV driving and uncoordinated charging

EV electricity consumption patterns can be derived from EV driving patterns. Based on a charging profile, these consumption patterns are further translated into charging patterns. The Netherlands Mobility Panel from the KiM Netherlands Institute for Transport Policy Analysis contains travel patterns for a representative sample population. This dataset contains 194,477 entries in the Netherlands between 2013 and 2016, categorized by start time and destination. These entries are used to calibrate a Markov chain model of EV locations and driving patterns (similar to that of [13]; details in Methods). Fig. 5 shows EV locations for a sample weekday. Most state changes are in the early morning and early evening hours, as drivers commute between home and work.

EVs discharge the energy stored in their batteries for these trips. The battery consumption patterns follow a similar diurnal pattern. Both travel and battery discharge also show weekly patterns, the latter of which is shown for a sample week in Fig. 6. During weekdays, commutes to and from work create large peaks in the early morning

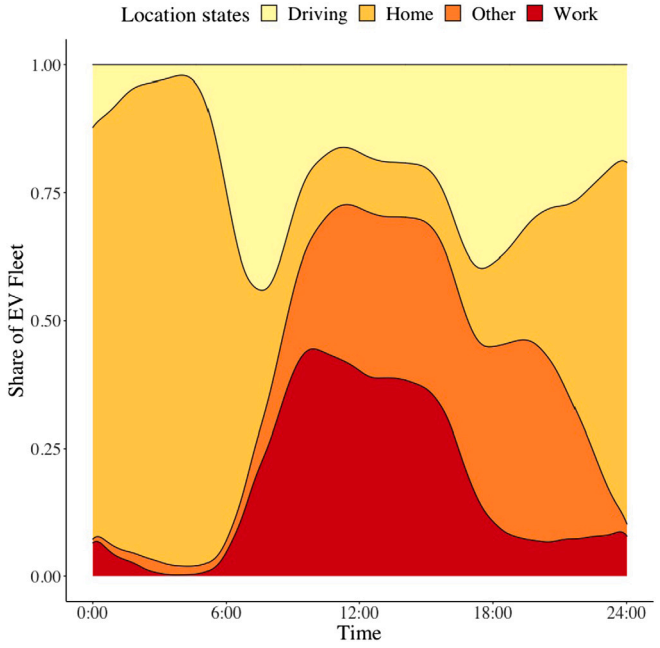

Fig. 5. EV location states throughout a day.

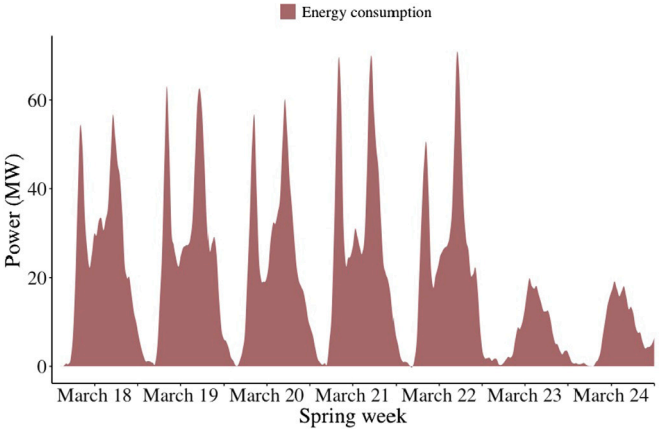

Fig. 6. EV energy consumption in the simulated spring week.

and evening hours, respectively. However, energy consumption during the weekends is far more limited.

Total EV discharging over a long time period, e.g. one week, can be considered equal to the total electricity used for EV charging (with energy transfer losses included). Based on the amount of EV and PV integration, these charging needs may be met with PV electricity generation. Fig. 7 compares total EV charging demand and total PV generation for different levels of PV integration and EV penetration in sample spring and winter weeks. In spring, there are very few configurations that would not allow for the EV charging demand to be met by PV generation. In winter, however, some low PV integration and high EV integration levels lead to a lower proportion of EV charging load being met by PV generation. In summer (not shown), all PV electricity generation over long time horizons is higher than the potential EV charging load. Generally, most if not all of EV charging can potentially be met by PV generation alone.

However, these aggregated analyses over long time horizons can be misleading. PV generation and EV discharging patterns vary dramatically on a minute-to-minute basis. More importantly, the relationship between EV travel (i.e. discharging) and charging is mediated by a hidden factor: how and when the EV is charged. Prior studies have used multiple strategies for EV charging, with three being the more common uncoordinated methods. The first strategy assumes opportunistic charging, where an EV user charges whenever and wherever possible [13]. The second assumes charging only at home after a day's travels are finished [42,51]. The third allows for charging whenever a car is parked for a minimum time span [43], in our case 2 h. Fig. 8 shows how well each strategy's charging matches discharging patterns. Strategy 3 is very similar in its charging pattern to Strategy 1, so we assume that opportunistic charging at any time is comparable to charging if the parking time exceeds two hours.

The matching between PV generation and EV charging can vary per strategy. Fig. 9 shows PV electricity generation and EV charging load (top) and their differences (bottom) for Strategy 1 in spring with 10% PV integration and 50% EV adoption (similar visualizations of sample weeks in winter and summer, as well as for Strategy 2 and 3, are included in Appendix 7.1.1.).[3] Referring back to Fig. 7, this sample indicates a setting that would, when time resolution is set to one week or more, suggest 85% coverage of EV charging with solar PV generation in spring, irrespective of charging strategy. However, the high-resolution perspective outlines that the actually realized solar charging from uncoordinated charging represents only a fraction of 85%.

When following uncoordinated charging strategies 1 and 3, EVs generally begin charging soon after driving ends. The south-facing panels create a midday PV generation peak that consistently exceeds charging load, leading to an energy surplus. The opposite is seen on weekdays during early morning and evening hours, as arrivals at work and home create energy deficit situations. Particularly large surpluses are seen during the weekends, when commuting to and from work is minimal. A different assumption may be that cars are charged upon arrival at home after the final trip of the day (Strategy 2). In this setting, PV generation, which is highest around noon, can be expected to poorly match EV charging, which is delayed until evening. As expected, Strategy 2's results (Fig. 18 in Appendix) are worse overall than Strategy 1's results (Fig. 9). Periods of electricity surplus and deficit are far larger in duration, average value, and peak value.

To quantify the comparisons between strategies, we use solar fractions as defined in Section 2.4. This metric is the share of the EV charging load that is met by corresponding PV generation. Fig. 10 shows the solar fraction values for the spring sample week for the first charging strategy. Compared to Fig. 7, the actual solar fraction values are far lower and far more dependent on PV and EV integration levels, charging strategy, and season. For the example of 50% EV penetration and 10% EV integration, the solar fraction reaches 45.6% instead of the value of 85% when disregarding temporal matching. These observations highlight the inherent volatility of solar irradiance and emphasize the importance of granular analysis rather than aggregating irradiance and charging demands across larger time horizons [10].

EV charging behavior is an additional determinant of the solar fraction. Comparing results for Strategy 1 and 2 (Appendix 7.1.2), we see that Strategy 1 generally shows higher solar fraction values than Strategy 2 across all PV and EV integration levels and seasons. Solar fraction values also differ across seasons. Higher solar irradiance and extended hours of sunlight in the summer months allow for a larger overlap between EV charging demand and solar energy availability. Furthermore, the solar peaks at midday tend to be higher in summer, leading to a larger coverage of EV charging needs through solar. As a result, summer leads to comparatively higher solar fraction values, while reduced solar intensity and time frames in winter lead to reduced

[3] The current rate of Rotterdam rooftops using solar panels is 2.2% [50]; thus 10% PV integration is closest to the most current case. 50% EV adoption is shown here to represent a middle ground in charging load.

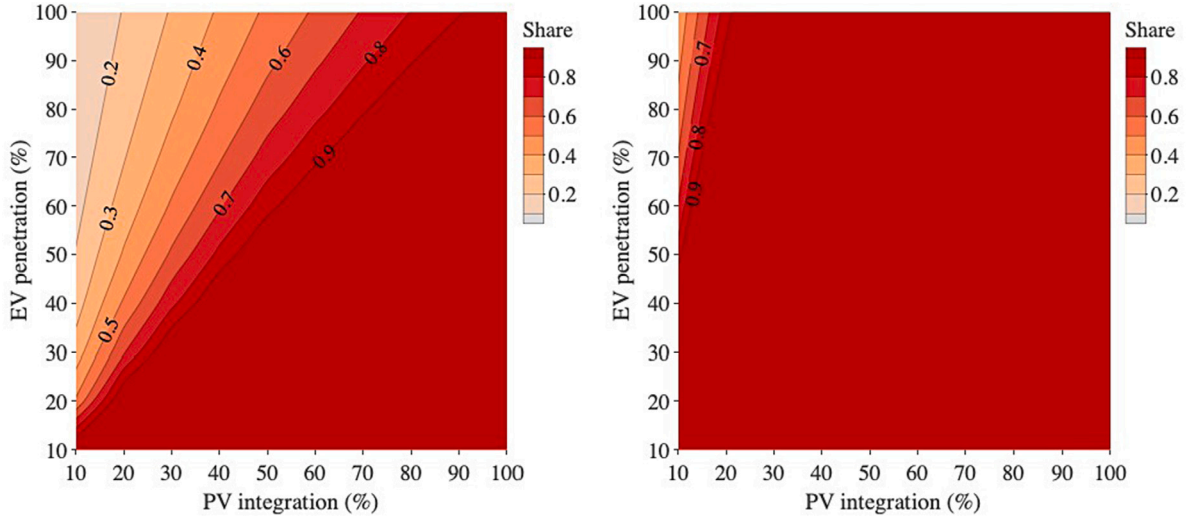

Fig. 7. PV generation share of EV charging per integration scenarios for sample weeks in winter (left) and spring (right).

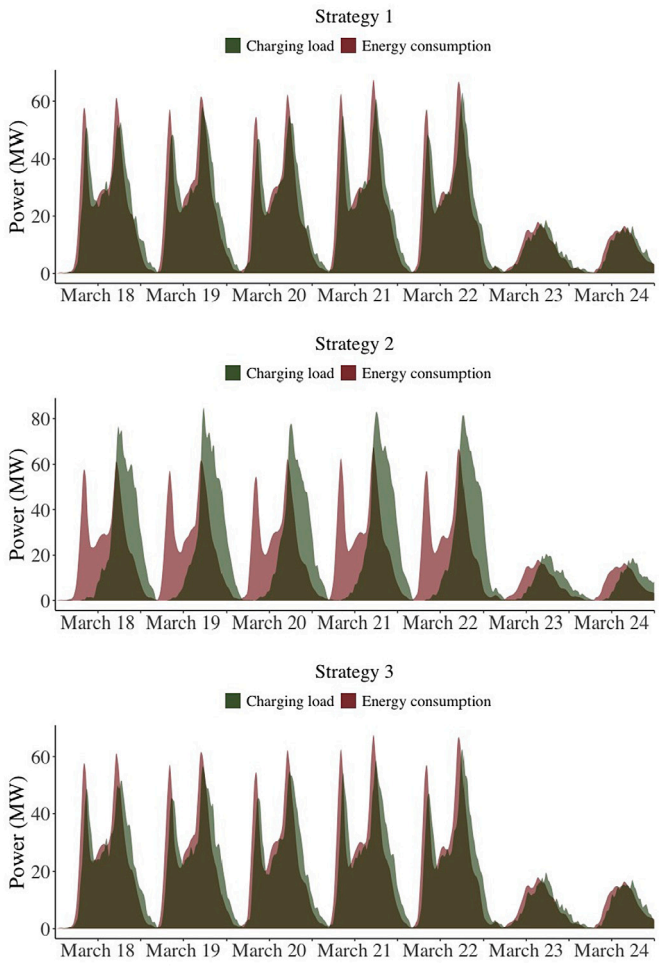

Fig. 8. Charging load and energy consumption across sample week for S1 (top), S2 (middle), S3 (bottom).

values. In the sample case with 50% EV penetration, 10% PV integration and charging at any time (strategy 1), a summer value of 62.4% compares to 45.6% and 14.4% for spring and winter, respectively.

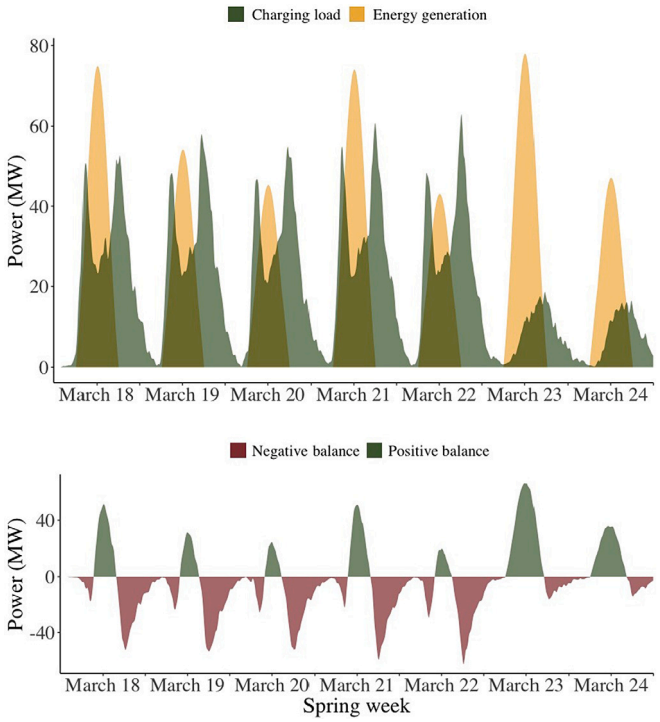

Fig. 9. Strategy 1: PV electricity generation and EV charging load (top) and their differences (bottom).

For comparison with prior research [13,48,49], we also investigated how much of PV generation is absorbed by EV charging, i.e. the load fraction. These results mirror solar fraction results and are included in Appendix 7.1.3.

5. Coordinating EV charging

The consideration of timing can significantly alter how much of an EV's energy requirements are met by PV generation [13]. Coordinating EV charging to better match PV generation trends can potentially improve solar fraction values and thus help solve the intermittency issue of solar energy [4,45]. The coordination mechanism prioritizes

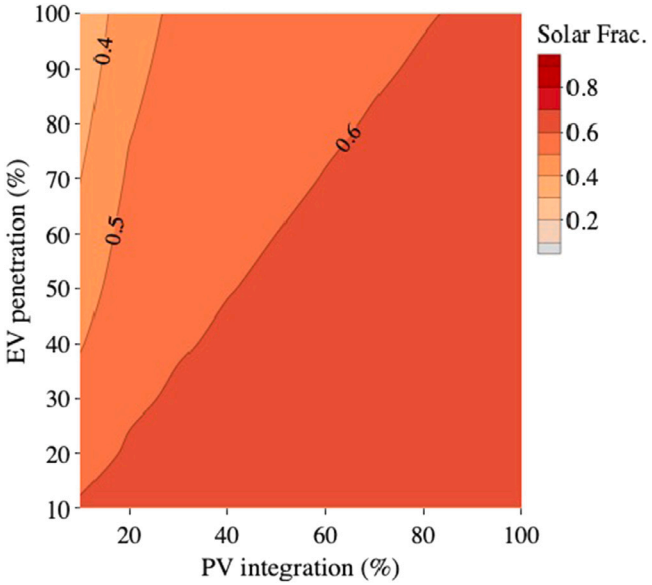

Fig. 10. Solar Fractions for first uncoordinated charging strategy in spring.

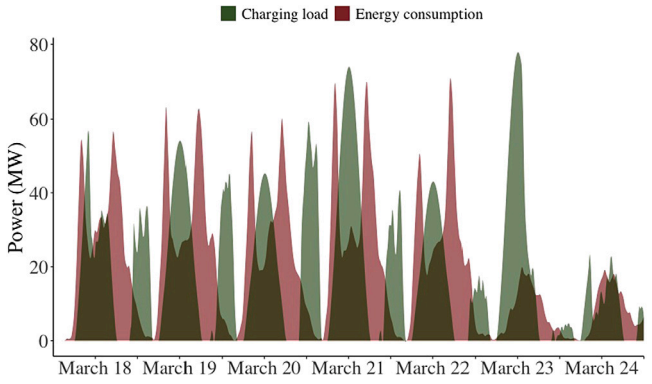

Fig. 11. EV energy consumption vs. coordinated charging.

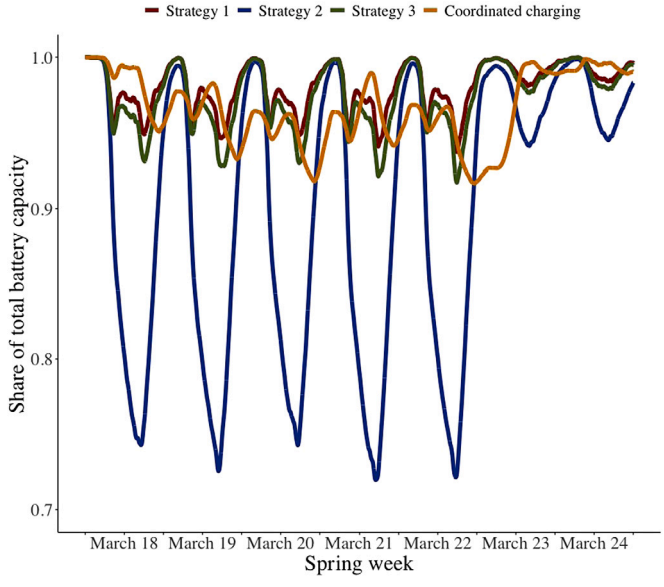

Fig. 12. Average charge levels.

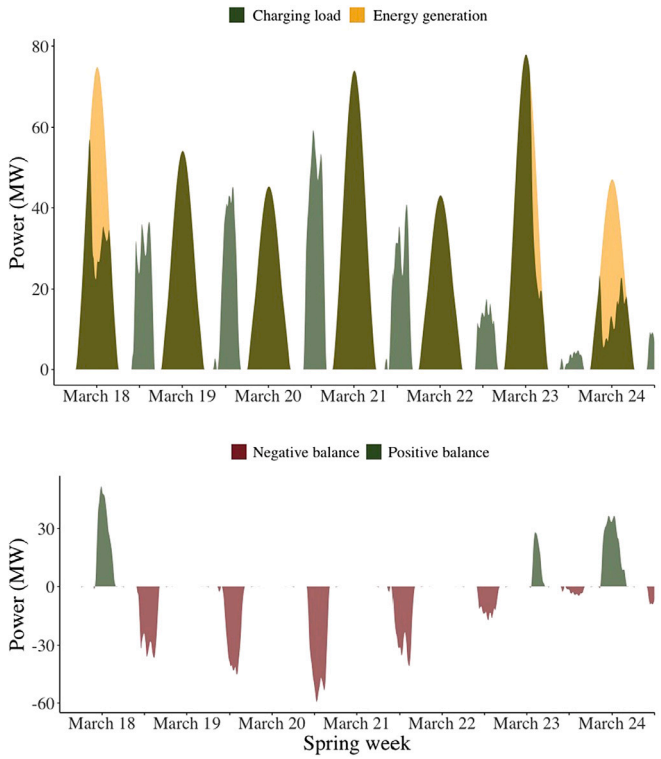

Fig. 13. Charging Load and Energy Generation for Strategy 4 (10% PV integration 50% EV integration).

charging EVs when solar energy is available (and charging is possible), and is only overridden if a critically low state of charge is predicted by the travel model.

Compared to the uncoordinated charging strategies, coordinated charging creates a large divergence between EV travel (battery discharge) and EV charging. Fig. 11 shows the distinct midday peak charges and additional night-time top-ups depending on necessity. These charging occasions are largely independent of actual EV energy consumption, which peaks in the morning and afternoon.

We can compare the various charging strategies to understand whether they are comparably unobtrusive for the driving preferences of EV owners in the long-term. Uncoordinated charging, particularly Strategy 1, place no restrictions on owner's charging, and thus maximize their potential battery charge at any given time. Coordinated charging, however, plans charging events based on the grid's preferences. Such prioritization could lead to the depletion of EV batteries in the long-run, leading to driver constraints. However, as Fig. 12 shows, coordinated charging leaves EV batteries with charging states similar to the uncoordinated strategies across the entire week. In the long-term, the coordinated charging strategy creates negligible constraints for travel for EV owners (we discuss short-term travel constraints later).

We next investigate the temporal match between PV generation and EV charging for charging strategy 4 (coordinated charging). Fig. 13 illustrates these results for a sample spring week with 10% PV and 50% EV integration. EV charging is centered around noontime and closely mirrors the distribution of PV electricity generation. Notable exceptions are the first weekday, when EV charging load is too low to absorb the significant solar PV generation and the last weekday, where the second day of reduced weekend EV consumption leads to excess solar energy.

The spikes in charging load between days represent non-solar night charging, required to charge the depleted batteries of cars which have a trip planned before 12pm the following day. They are indicative of an unavoidable temporal mismatch between solar availability and EV charging load, as well as a total energy deficit of 15% of the

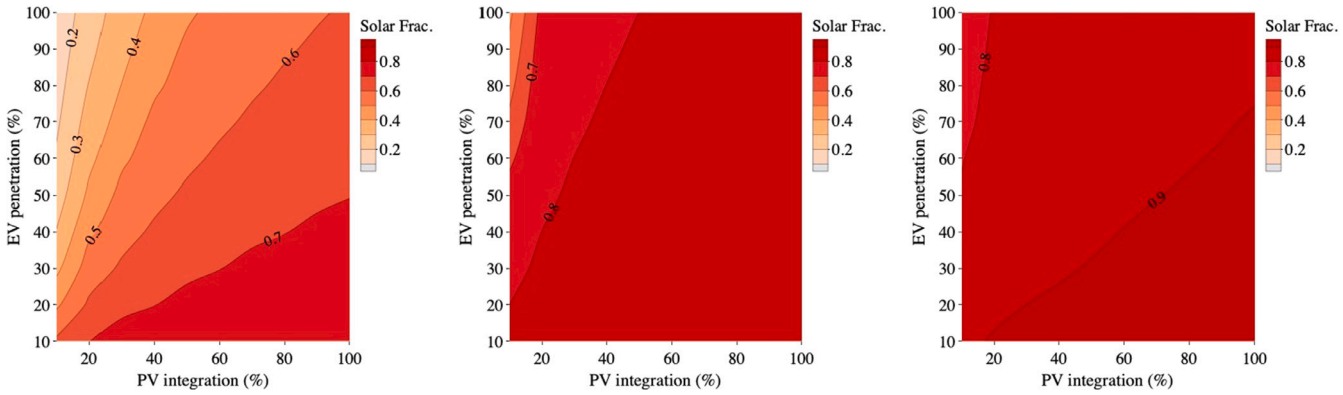

Fig. 14. Solar Fraction values with coordinated charging for winter (l), spring (c) and summer (r).

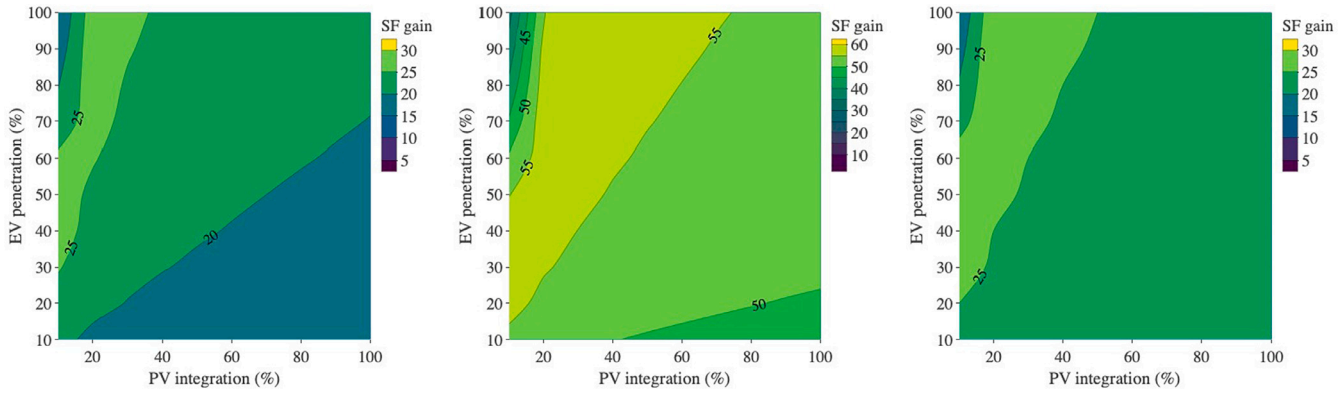

Fig. 15. Solar Fraction gain in pp from coordinated charging compared to S1 (l), S2 (c), S3 (r) in spring.

total EV energy consumption in a sample week in spring (with 10% PV integration and 50% EV penetration). Night-time charging appears to significantly increase after weekdays with reduced solar irradiance (Tuesday and Thursday in our sample).[4]

We next compare solar fraction values in coordinated charging across PV and EV integration levels and seasons, as shown in Fig. 14. All EV and PV integration levels in the spring are associated with solar fraction values above 80%, with a few exceptions in case of high EV and low PV integration. In the extreme case of 100% EV penetration and a corresponding PV integration of 10%, the solar fraction drops to 45%. In EV/PV penetration combinations which lead to considerable energy surplus, the solar fraction does not exceed 84%. In winter, solar fraction values are significantly reduced, ranging from merely 12.6% (10% PV and 100% EV) to 75.8% (100% PV and 10% EV). During summer, the extended window of daylight drives up the solar fraction to consistently high values, ranging from 70.6% to 91.6% for the respective cases. Nevertheless, a solar fraction of 100% remains elusive. This divergence from full solar charging is "unavoidable" with such coordination in charging, unless EV availability for drivers is entirely ignored. Including external batteries or V2G (Vehicle-to-Grid) technology, which renders an EV capable of storing electricity and later feeding it back into the grid [8], also bridges the temporal mismatch between solar availability and charging needs and could enable an increase in the solar fraction towards 100%.

Our main research interest is in comparing the coordinated charging strategy (4) with the uncoordinated strategies (1–3) in how they match PV generation and EV charging. Fig. 15 shows solar fraction gains between these strategies for spring (Appendix 7.2.2 contains plots for summer and winter seasons). Compared to uncoordinated charging at any time (Strategy 1) and when cars are stopped for longer than two hours (Strategy 3), coordinated charging enables solar fraction increases of 15–29 percentage points (pp) in spring. Compared with end-of-day charging (Strategy 2), solar fractions are increased by more than 33 pp, up to almost 58 pp. Similar results for load fraction were calculated and are included in Appendix 7.2.3. A comparison of energy utilization across all strategies in spring for 50% EV integration and 10% PV integration is presented in Table 5.

An important consideration for coordinating EV charging is its effect on the EV's availability for the driver. Coordinated charging is designed to de-prioritize EV availability and instead prioritize the matching of charging patterns with PV generation. The night-time charging ensures all drivers have enough battery for their next-day trips and thus minimizes occurrences where drivers need to make charging stops during a drive. In the Strategy 4 sample discussed above, with 10% PV and 50% EV integration for a sample spring week, merely 0.5% of drivers needed to stop during a ride to recharge a critically low battery. Even in an unfavorable winter scenario with only 10% PV integration and 70% EV penetration, only 2.1% of the EV drivers incur a delay and thus are negatively impacted by prioritizing solar availability. Hence, the coordinated charging strategy used here has a negligible impact on the EV's availability to the driver.

In summary, we find that coordinating EV charging strongly increases the amount of solar PV generation absorbed by EV energy consumption. These results vary significantly with season, with higher solar fractions in the summer and lower values in the winter. Yet coordinated charging bears significant gains across all seasons when compared with any form of opportunistic charging. These improvements sacrifice EV availability for drivers, which are only marginally relevant in low PV integration scenarios in winter.

[4] Seasonality also affects the charging patterns for Strategy 4. The night-charging peaks are more prominent in winter times, as fewer cars receive the necessary energy during the day. In summer, the night charging peaks are significantly lower (A comparison of the 50% EV and 10% PV scenario for winter, spring and summer is depicted in Appendix 7.2.1).

Table 5
Energy comparison across strategies (sample week in spring with 50% EV integration and 10% PV integration; columns 2,3, and 4 in MWh, columns 5 and 6 in %).

Charg. Strat.	EV load[a]	Sol. char.	Non-sol. char.	Solar Frac.	Load Frac.
(1) Whenever, wherever	3328.1	1516.6	1811.5	53.6	45.6
(2) End-of-day	3314.6	615.2	2699.4	21.7	18.6
(3) Prolonged Parking	3326.7	1473.8	1852.9	52.1	44.3
(4) Coordinated	3285.8	2431.5	854.4	74.0	85.9

[a]Divergence due to minor differences in charging states at midnight at week's end

6. Conclusions

With the rapid increase in PVs and EVs in many regions across the world, the challenges of integrating one may be solved by opportunities created by the other. Unlike most traditional generation resources, solar units are uncontrollable in their electricity production. EVs are also unlike most other electricity consumption sinks, as the battery detaches energy consumption (driving) from grid use (charging). Thus, the consumption needs of EVs can be adjusted to match the uncontrollable nature of PV generation. Ignoring the temporal constraints of PV generation and EV charging could misleadingly dilute the benefits from EV charging coordination and present unreasonably high benefits to matching. Considering the temporal constraints, we show that this matching is possible over most ranges of PV and EV integration with minimal disruption to EV users. In particular, we show how a simple coordination mechanism can drastically improve outcomes compared to generic uncoordinated charging behaviors, such as charging whenever a car parks or charging at a day's end. This gain does not come at a significant cost of EV availability for drivers.

Similar to prior research [13,52], we find that opportunistic (uncoordinated) charging leads to low amounts of solar energy being absorbed by EV batteries. Even in scenarios with significant solar energy surplus (e.g. PV generation producing 426% of EV charging requirements in a scenario of 50% EV and 50% PV penetration) the share of solar energy of the entire charge (solar fraction) represents merely 60.8%, 27.4%, and 58.0%, for the uncoordinated charging strategies 1 (charging whenever), 2 (charging at day's end), and 3 (charging when parked for over 2 hours), respectively. This divergence is primarily due to the difference of charging peaks (in morning and late afternoon) from midday solar peaks and only appears when high time granularity is used. This granularity depends not only on the modeling choices, but also on the availability of such granularity in the dataset.

With the simple coordination mechanism, we find that EVs can absorb far higher ratios of solar PV generation. In the aforementioned scenario with abundant solar availability (and a maximum potential solar fraction of 85%), the solar fraction totals 82.4% - a gain of 22, 55, and 24 percentage points in the share of solar energy compared to strategy 1, 2, and 3, respectively. This coordination mechanism generally works well for all seasons. Surprisingly, the proportionate gains of coordinated charging over uncoordinated charging is highest in winter scenarios. Due to the low solar fractions in winter, the gain ratio is calculated on top of a smaller denominator, leading to a proportionally larger gain in winter. In absolute terms, however, the gain in solar energy used for EV charging by strategy 4 is highest in summer (when available solar energy is highest).

Our findings emphasize the immense potential of charging coordination for the efficient utilization of solar energy. As such, the proposed solution can complement other solar solutions. Coordination can increase the viability of building-integrated photovoltaic systems (BIPVs), which are found to be environmentally and economically beneficial [53] and thus are promising in cities where rooftop solutions might be less feasible. The proposed coordination solution does not interfere with but rather complements other solar solutions. When integrating with entire household systems, this solution also benefits the integration of non-photovoltaic solar solutions, such as traditional solar thermal technology [54] and newer Solar Thermally Activated Façade (STAF) panels [55]. Thus, charging coordination together with city-scale rooftop solar photovoltaic generation can complement existing as well as future solar solutions and thereby catalyzes the adoption of renewable energy sources.

6.1. Limitations and future work

Although derived for the Dutch city of Rotterdam, the findings and especially the temporal benefit of charging coordination can be extrapolated to cities of similar population density, topography, and latitude. Generally, cities at lower latitudes would experience smaller differences across seasons. The immense coordination gains in the winter scenarios underline the potential for latitudes which experience seasons of extremely short windows of daily sunlight. Given data availability, our study's methodology can be similarly applied to other cities that may differ significantly from our sample case. It would be particularly interesting to apply these methods to cities with differing road networks and modes of transport, such as larger Asian metropolises.

This study examines direct charging of EV batteries with solar energy. Energy storage between the two, e.g. stationary batteries, has been omitted in this study. These technologies contain much potential for increasing solar and load fractions [13,56]. In this regard, V2G or V2H (Vehicle-to-Home) technologies, can utilize EVs as decentralized energy storage for locally generated excess power and thereby introduce additional flexibility to the energy system [4,57]. However, these technologies require additional hardware and impose other unique challenges for transmission and distribution networks [45,58]. This limited viability discouraged us from considering V2G energy transfers. Furthermore, our study does not include the behavioral aspects of EV charging. Previous studies have for instance considered household energy demand and its correlation with EV charging loads [49,59]. A comprehensive study may include both behavioral factors and their influence on electricity demand to assess matching with PV generation. On the supply side, our study's focus on the city scale prevents us from considering synergies between PVs and other RES generation. Particularly at night time when solar energy dips, wind energy could be a suitable alternative [60]. Further research can study these synergies and their influences on increasing matching with EV energy consumption.

CRediT authorship contribution statement

Ulrich Fretzen: Conceptualization, Methodology, Software, Validation, Formal analysis, Data curation, Writing. **Mohammad Ansarin:** Conceptualization, Methodology, Software, Validation, Formal analysis, Writing, Supervision. **Tobias Brandt:** Conceptualization, Methodology, Validation, Writing, Supervision.

Declaration of competing interest

The authors declare that they have no known competing financial interests or personal relationships that could have appeared to influence the work reported in this paper.

Appendix A. Supplementary data

Supplementary material related to this article can be found online at https://doi.org/10.1016/j.apenergy.2020.116160.

References

[1] European Environment Agency. Annual European Union greenhouse gas inventory 1990–2017 and inventory report 2019, no. May. 2019, p. 962.

[2] Zahedi A. Maximizing solar PV energy penetration using energy storage technology. Renew Sustain Energy Rev 2011;15(1):866–70. http://dx.doi.org/10.1016/j.rser.2010.09.011.

[3] Beaufils T, Pineau PO. Assessing the impact of residential load profile changes on electricity distribution utility revenues under alternative rate structures. Util Policy 2019;61(August):100959. http://dx.doi.org/10.1016/j.jup.2019.100959.

[4] Fattori F, Anglani N, Muliere G. Combining photovoltaic energy with electric vehicles, smart charging and vehicle-to-grid. Sol Energy 2014;110:438–51. http://dx.doi.org/10.1016/j.solener.2014.09.034.

[5] Cairns EJ, Albertus P. Batteries for electric and hybrid-electric vehicles. Annu Rev Chem Biomol Eng 2010;1(1):299–320. http://dx.doi.org/10.1146/annurev-chembioeng-073009-100942.

[6] Reininger C, Salmon J. Systems feasibility study for implementing electric vehicles into urban environments. 9th annual IEEE international systems conference, SysCon 2015 - Proceedings 2015;734–9. http://dx.doi.org/10.1109/SYSCON.2015.7116838.

[7] International Energy Agency I. Towards cross-modal electrification Global EV outlook 2018. Tech. rep., IEA; 2018, http://dx.doi.org/10.1787/9789264302365-en.

[8] Richardson DB. Electric vehicles and the electric grid: A review of modeling approaches, impacts, and renewable energy integration. Renew Sustain Energy Rev 2013;19:247–54. http://dx.doi.org/10.1016/j.rser.2012.11.042.

[9] Ul-Haq A, Cecati C, El-Saadany E. Probabilistic modeling of electric vehicle charging pattern in a residential distribution network. Electr Power Syst Res 2018;157:126–33. http://dx.doi.org/10.1016/J.EPSR.2017.12.005, URL https://www-sciencedirect-com.eur.idm.oclc.org/science/article/pii/S0378779617304765?via%3Dihub.

[10] Shepero M, Munkhammar J, Widén J, Bishop JD, Boström T. Modeling of photovoltaic power generation and electric vehicles charging on city-scale: A review. Renew Sustain Energy Rev 2018;89(March):61–71. http://dx.doi.org/10.1016/j.rser.2018.02.034.

[11] Chaouachi A, Bompard E, Fulli G, Masera M, De Gennaro M, Paffumi E. Assessment framework for EV and PV synergies in emerging distribution systems. Renew Sustain Energy Rev 2016;55:719–28. http://dx.doi.org/10.1016/j.rser.2015.09.093.

[12] Shepero M, Lingfors D, Widén J, Bright JM, Munkhammar J. Estimating the spatiotemporal potential of self-consuming photovoltaic energy to charge electric vehicles in rural and urban nordic areas. J Renew Sustain Energy 2020;12(4). http://dx.doi.org/10.1063/5.0006893.

[13] Good C, Shepero M, Munkhammar J, Boström T. Scenario-based modelling of the potential for solar energy charging of electric vehicles in two Scandinavian cities. Energy 2018;168:111–25. http://dx.doi.org/10.1016/j.energy.2018.11.050, URL https://www.sciencedirect.com/science/article/pii/S0360544218322540?dgcid=raven_sd_aip_email.

[14] Kostopoulos E, Spyropoulos G, Christopoulos K, Kaldellis JK. Solar energy contribution to an electric vehicle needs on the basis of long-term measurements. Procedia Struct Integr 2018;10:203–10. http://dx.doi.org/10.1016/j.prostr.2018.09.029.

[15] Neumann H-M, Schär D, Baumgartner F. The potential of photovoltaic carports to cover the energy demand of road passenger transport. Progr Photovolt 2011;(October 2011):639–49. http://dx.doi.org/10.1002/pip.

[16] Birnie DP. Solar-to-vehicle (S2V) systems for powering commuters of the future. J Power Sources 2009;186(2):539–42. http://dx.doi.org/10.1016/j.jpowsour.2008.09.118, URL https://linkinghub.elsevier.com/retrieve/pii/S0378775308018946.

[17] Ul-Haq A, Azhar M, Mahmoud Y, Perwaiz A, Al-Ammar EA. Probabilistic modeling of electric vehicle charging pattern associated with residential load for voltage unbalance assessment. Energies 2017;10(9):1–18. http://dx.doi.org/10.3390/en10091351.

[18] Rolink J, Rehtanz C. Large-scale modeling of grid-connected electric vehicles. IEEE Trans Power Deliv 2013;28(2):894–902. http://dx.doi.org/10.1109/TPWRD.2012.2236364, URL http://ieeexplore.ieee.org/document/6423232/.

[19] Wu D, Aliprantis DC, Gkritza K. Electric energy and power consumption by light-duty plug-in electric vehicles. IEEE Trans Power Syst 2011;26(2):738–46. http://dx.doi.org/10.1109/TPWRS.2010.2052375, URL http://ieeexplore.ieee.org/document/5524052/.

[20] Rassaei F, Soh WS, Chua KC. Demand response for residential electric vehicles with random usage patterns in smart grids. IEEE Trans Sustain Energy 2015;6(4):1367–76. http://dx.doi.org/10.1109/TSTE.2015.2438037.

[21] Li D, Zouma A, Liao J-T, Yang H-T. An energy management strategy with renewable energy and energy storage system for a large electric vehicle charging station. eTransportation 2020;6:100076. http://dx.doi.org/10.1016/j.etran.2020.100076.

[22] Spitzer M, Schlund J, Apostolaki-Iosifidou E, Pruckner M. Optimized integration of electric vehicles in low voltage distribution grids. Energies 2019;12(21):1–19. http://dx.doi.org/10.3390/en12214059.

[23] Muratori M. Impact of uncoordinated plug-in electric vehicle charging on residential power demand. Nat Energy 2018;3(3):193–201. http://dx.doi.org/10.1038/s41560-017-0074-z, URL http://www.nature.com/articles/s41560-017-0074-z.

[24] Will C, Schuller A. Understanding user acceptance factors of electric vehicle smart charging. Transp Res C 2016;71:198–214. http://dx.doi.org/10.1016/j.trc.2016.07.006.

[25] Lukač N, Seme S, Žlaus D, Štumberger G, Žalik B. Buildings roofs photovoltaic potential assessment based on LiDAR (Light Detection And Ranging) data. Energy 2014;66:598–609. http://dx.doi.org/10.1016/J.ENERGY.2013.12.066, URL https://www.sciencedirect.com/science/article/pii/S0360544213011365.

[26] Ko Y, Jang K, Radke JD. Toward a solar city: Trade-offs between on-site solar energy potential and vehicle energy consumption in san francisco, california. Int J Sustain Transp 2017;11(6):460–70. http://dx.doi.org/10.1080/15568318.2016.1274807.

[27] Kodysh JB, Omitaomu OA, Bhaduri BL, Neish BS. Methodology for estimating solar potential on multiple building rooftops for photovoltaic systems. Sustainable Cities Soc 2013;8:31–41. http://dx.doi.org/10.1016/j.scs.2013.01.002, URL https://www.sciencedirect.com/science/article/pii/S2210670713000036.

[28] Pecan Street. GreenTech Media: Are solar panels facing the wrong direction? – Pecan Street Inc. 2013, URL https://www.pecanstreet.org/2013/11/are-solar-panels-facing-the-wrong-direction/.

[29] Wang Y, Infield D. Markov Chain Monte Carlo simulation of electric vehicle use for network integration studies. Int J Electr Power Energy Syst 2018;99:85–94. http://dx.doi.org/10.1016/J.IJEPES.2018.01.008, URL https://www-sciencedirect-com.eur.idm.oclc.org/science/article/pii/S0142061517307226?via%3Dihub.

[30] Grana P. The new rules for latitude and solar system design. 2018, URL https://www.solarpowerworldonline.com/2018/08/new-rules-for-latitude-and-solar-system-design/.

[31] Aguiar RJ, Collares-Pereira M, Conde JP. Simple procedure for generating sequences of daily radiation values using a library of Markov transition matrices. Sol Energy 1988;40(3):269–79. http://dx.doi.org/10.1016/0038-092X(88)90049-7, URL https://linkinghub.elsevier.com/retrieve/pii/0038092X88900497.

[32] Mckay DC. Estimating solar irradiance on inclined surfaces: A review and assessment of methodologies. Int J Sol Energy 1985;3(4–5):203–40. http://dx.doi.org/10.1080/01425918508914395.

[33] Martin N, Ruiz JM. Calculation of the PV modules angular losses under field conditions by means of an analytical model. Sol Energy Mater Sol Cells 2001;70(1):25–38. http://dx.doi.org/10.1016/S0927-0248(00)00408-6.

[34] Byrne J, Taminiau J, Kurdgelashvili L, Kim KN. A review of the solar city concept and methods to assess rooftop solar electric potential, with an illustrative application to the city of Seoul. Renew Sustain Energy Rev 2015;41:830–44. http://dx.doi.org/10.1016/j.rser.2014.08.023.

[35] Koralov L, Sinai YG. Theory of probability and random processes. Universitext, Berlin, Heidelberg: Springer Berlin Heidelberg; 2007, http://dx.doi.org/10.1007/978-3-540-68829-7, URL http://link.springer.com/10.1007/978-3-540-68829-7.

[36] Widén J, Wäckelgård E, Lund PD. Options for improving the load matching capability of distributed photovoltaics: Methodology and application to high-latitude data. Sol Energy 2009;83(11):1953–66. http://dx.doi.org/10.1016/j.solener.2009.07.007, URL https://linkinghub.elsevier.com/retrieve/pii/S0038092X09001741.

[37] Soares F, Lopes J. A stochastic model to simulate electric vehicles motion and quantify the energy required from the grid. In: 17th power systems computation conference. (1):2011, p. 7. http://dx.doi.org/10.1007/978-3-322-94390-3, URL http://www.pscc-central.org/uploads/tx_ethpublications/fp359.pdf.

[38] Shepero M, Munkhammar J. Modelling charging of electric vehicles using mixture of user behaviours. In: 1st e-mobility power system integration symposium, Berlin, Germany, 23 October 2017. 2017, http://mobilityintegrationsymposium.org/berlin2017/wp-content/uploads/sites/7/2018/06/EMob17_034_posterpaper_Shepero_Mahmoud.pdf.

[39] Netherlands Enterprise Agency. Statistics electric vehicles in the netherlands number of electric vehicles on the road in The Netherlands (fleet) 2, no. august. 2018, URL https://www.government.nl/ministries/ministry-of-infrastructure-and-water-management.

[40] Spoelstra JC. Charging behaviour of Dutch EV drivers: A study into the charging behaviour of Dutch EV drivers and factors that influence this behaviour. 2014.

[41] Denholm P, Kuss M, Margolis RM. Co-benefits of large scale plug-in hybrid electric vehicle and solar PV deployment. J Power Sources 2013;236:350–6. http://dx.doi.org/10.1016/j.jpowsour.2012.10.007, URL https://linkinghub.elsevier.com/retrieve/pii/S0378775312015534.

[42] Falahati S, Taher SA, Shahidehpour M. A new smart charging method for EVs for frequency control of smart grid. Int J Electr Power Energy Syst 2016;83:458–69. http://dx.doi.org/10.1016/J.IJEPES.2016.04.039, URL https://www-sciencedirect-com.eur.idm.oclc.org/science/article/pii/S0142061516307244.

[43] Shepero M, Munkhammar J. Spatial Markov chain model for electric vehicle charging in cities using geographical information system (GIS) data. Appl Energy 2018;231(June):1089–99. http://dx.doi.org/10.1016/j.apenergy.2018.09.175.

[44] Peças Lopes JA, Soares FJ, Rocha Almeida PM. Identifying management procedures to deal with connection of electric vehicles in the grid. In: 2009 IEEE bucharest powertech: Innovative ideas towards the electrical grid of the future. 2009, p. 1–8. http://dx.doi.org/10.1109/PTC.2009.5282155.

[45] Solanke TU, Ramachandaramurthy VK, Yong JY, Pasupuleti J, Kasinathan P, Rajagopalan A. A review of strategic charging–discharging control of grid-connected electric vehicles. J Energy Storage 2020;28(January):101193. http://dx.doi.org/10.1016/j.est.2020.101193.

[46] Pecas Lopes JA, Soares FJ, Almeida PM, Moreira Da Silva M. Smart charging strategies for electric vehicles: Enhancing grid performance and maximizing the use of variable renewable energy resources. In: BT - 24th international battery, hybrid and fuel cell electric vehicle symposium and exhibition 2009, EVS 24, May 13, vol. 4, no. February 2014; 2009. p. 2680–90.

[47] Bae S, Kwasinski A. Spatial and temporal model of electric vehicle charging demand. IEEE Trans Smart Grid 2012;3(1):394–403. http://dx.doi.org/10.1109/TSG.2011.2159278, URL http://ieeexplore.ieee.org/document/5959242/.

[48] Luthander R, Widén J, Nilsson D, Palm J. Photovoltaic self-consumption in buildings: A review. Appl Energy 2015;142:80–94. http://dx.doi.org/10.1016/j.apenergy.2014.12.028.

[49] Munkhammar J, Grahn P, Widén J. Quantifying self-consumption of on-site photovoltaic power generation in households with electric vehicle home charging. Sol Energy 2013;97:208–16. http://dx.doi.org/10.1016/j.solener.2013.08.015.

[50] Sobolt. Solar suitability in Rotterdam. Tech. rep., Rotterdam; 2019.

[51] Wang X, Karki R. Exploiting PHEV to augment power system reliability. IEEE Trans Smart Grid 2017;8(5):2100–8. http://dx.doi.org/10.1109/TSG.2016.2515989.

[52] van der Kam M, van Sark W. Smart charging of electric vehicles with photovoltaic power and vehicle-to-grid technology in a microgrid; a case study. Appl Energy 2015;152:20–30. http://dx.doi.org/10.1016/j.apenergy.2015.04.092.

[53] Gholami H, Røstvik HN. Economic analysis of BIPV systems as a building envelope material for building skins in Europe. Energy 2020;204:117931. http://dx.doi.org/10.1016/j.energy.2020.117931.

[54] Hansen K, Vad Mathiesen B. Comprehensive assessment of the role and potential for solar thermal in future energy systems. Sol Energy 2018;169(January):144–52. http://dx.doi.org/10.1016/j.solener.2018.04.039.

[55] Strušnik D, Brandl D, Schober H, Ferčec J, Avsec J. A simulation model of the application of the solar STAF panel heat transfer and noise reduction with and without a transparent plate: A renewable energy review. Renew Sustain Energy Rev 2020;134(July). http://dx.doi.org/10.1016/j.rser.2020.110149.

[56] Nyholm E, Goop J, Odenberger M, Johnsson F. Solar photovoltaic-battery systems in Swedish households – self-consumption and self-sufficiency. Appl Energy 2016;183:148–59. http://dx.doi.org/10.1016/j.apenergy.2016.08.172.

[57] Kempton W, Tomić J. Vehicle-to-grid power implementation: From stabilizing the grid to supporting large-scale renewable energy. J Power Sources 2005;144(1):280–94. http://dx.doi.org/10.1016/j.jpowsour.2004.12.022.

[58] Kempton W, Tomić J. Vehicle-to-grid power fundamentals: Calculating capacity and net revenue. J Power Sources 2005;144(1):268–79. http://dx.doi.org/10.1016/j.jpowsour.2004.12.025.

[59] Paevere P, Higgins A, Ren Z, Horn M, Grozev G, McNamara C. Spatio-temporal modelling of electric vehicle charging demand and impacts on peak household electrical load. Sustain Sci 2014;9(1):61–76. http://dx.doi.org/10.1007/s11625-013-0235-3, URL http://link.springer.com/10.1007/s11625-013-0235-3.

[60] Zhang H, Cao Y, Zhang Y, Terzija V. Quantitative synergy assessment of regional wind-solar energy resources based on MERRA reanalysis data. Appl Energy 2018;216:172–82. http://dx.doi.org/10.1016/j.apenergy.2018.02.094, URL https://linkinghub.elsevier.com/retrieve/pii/S0306261918302198.